Biomaterials 31 (2010) 5372–5384

Contents lists available at ScienceDirect

Biomaterials

journal homepage: www.elsevier.com/locate/biomaterials

Delivery of paclitaxel from cobalt–chromium alloy surfaces without polymeric carriers

Gopinath Mani [a,*], Celia E. Macias [a], Marc D. Feldman [a,b,c], Denes Marton [a,d], Sunho Oh [a], C. Mauli Agrawal [a]

[a] Department of Biomedical Engineering, College of Engineering, The University of Texas at San Antonio, One UTSA Circle, San Antonio, TX 78249-0619, USA
[b] Division of Cardiology, Department of Medicine, The University of Texas Health Science Center at San Antonio, 7703 Floyd Curl Drive, San Antonio, TX 78229-3900, USA
[c] The Department of Veterans Affairs South Texas Health Care System, San Antonio, TX 78229-4404, USA
[d] Department of Radiology, School of Medicine, The University of Texas Health Science Center at San Antonio, 7703 Floyd Curl Drive, San Antonio, TX 78229-3900, USA

ARTICLE INFO

Article history:
Received 5 February 2010
Accepted 16 March 2010
Available online 15 April 2010

Keywords:
Drug-eluting stents
Drug delivery
Cobalt–Chromium alloy
Surface treatment
Surface modification

ABSTRACT

Polymer-based carriers are commonly used to deliver drugs from stents. However, adverse responses to polymer coatings have raised serious concerns. This research is focused on delivering drugs from stents without using polymers or any carriers. Paclitaxel (PAT), an anti-restenotic drug, has strong adhesion towards a variety of material surfaces. In this study, we have utilized such natural adhesion property of PAT to attach these molecules directly to cobalt–chromium (Co–Cr) alloy, an ultra-thin stent strut material. Four different groups of drug coated specimens were prepared by directly adding PAT to Co–Cr alloy surfaces: Group-A (PAT coated, unheated, and ethanol cleaned); Group-B (PAT coated, heat treated, and ethanol cleaned); Group-C (PAT coated, unheated, and not ethanol cleaned); and Group-D (PAT coated, heat treated and not ethanol cleaned). *In vitro* drug release of these specimens was investigated using high performance liquid chromatography. Groups A and B showed sustained PAT release for up to 56 days. A simple ethanol cleaning procedure after PAT deposition can remove the loosely bound drug crystals from the alloy surfaces and thereby allowing the remaining strongly bound drug molecules to be released at a sustained rate. The heat treatment after PAT coating further improved the stability of PAT on Co–Cr alloy and allowed the drug to be delivered at a much slower rate, especially during the initial 7 days. The specimens which were not cleaned in ethanol, Groups C and D, showed burst release. PAT coated Co–Cr alloy specimens were thoroughly characterized using scanning electron microscopy, atomic force microscopy, and X-ray photoelectron spectroscopy. These techniques were collectively useful in studying the morphology, distribution, and attachment of PAT molecules on Co–Cr alloy surfaces. Thus, this study suggests the potential for delivering paclitaxel from Co–Cr alloy surfaces without using any carriers.

1. Introduction

Atherosclerotic disease of the coronary arteries can lead to myocardial infarction (heart attack) [1]. Atherosclerosis can be treated using implantation of metal stents which opens up the artery and restores blood flow to the heart [2,3]. However, stent deployment often involves damage to the arterial wall and causes secondary neointimal hyperplasia [4]. Neointimal hyperplasia is primarily characterized by migration and growth of smooth muscle cells followed by extracellular matrix synthesis and deposition resulting in re-occlusion of the lumen [5]. Drug-eluting stents (DES), which release drugs to inhibit the growth and secretion of smooth muscle cells, are currently used to effectively treat this condition [6,7]. Although the results of short-term clinical trials of DES demonstrate their usefulness, the long-term trials showed risks of late stent thrombosis with adverse clinical events [8–10]. Polymer-based drug delivery carriers in stents have been shown to cause adverse reactions in patients [11–15]. Also, polymers interfere with the blood vessel's normal healing process and are considered to be a major factor in very late thrombosis [8,9]. Hence, several alternate techniques are under development to deliver drugs from stents without using polymers [16–25].

The non-polymer based drug delivery platforms available for coronary stents can generally be classified under two different

* Corresponding author. Tel.: +1 210 458 5081; fax: +1 210 458 7007.
E-mail address: Gopinath.Mani@utsa.edu (G. Mani).

0142-9612/$ – see front matter © 2010 Elsevier Ltd. All rights reserved.
doi:10.1016/j.biomaterials.2010.03.043

categories, physical and chemical modification of stent surfaces. The physical modification of stents includes porous, textured, and reservoir surfaces [26]. The chemical modification includes the use of molecular coatings such as self-assembled monolayers [22,23]. Porous stents with different sizes of pores (nanopores – 1 to 100 nm; micropores – 1 to 100 μm; macropores – greater than 100 μm) have been created for loading and releasing the drugs directly from stent surfaces [21]. Nanoporous surfaces have been created by coating the stents first with a thin layer of aluminum followed by electrochemical conversion of aluminum to nanoporous aluminum oxide [16]. However, the particle debris liberated from such ceramic coated stents has caused serious adverse reactions in an animal model [27]. Nanoporous metals [28] and carbon-carbon nanoparticle coatings [18] have also been previously explored for delivering drugs directly from stent surfaces. Micro-textured surfaces have been created on stents by sandblasting treatment [17]. Although the clinical performance of sandblasted stents is encouraging, the on-site loading of drugs in clinics prior to stent implantation may not be a favorable approach. Reservoir surfaces have been created by laser cut holes on stent struts and the holes were subsequently filled with drugs. However, the clinical outcomes of such stents were not significantly different from their control groups [20]. The use of self-assembled monolayers for delivering drugs from metal surfaces is also promising [22,23] and currently under investigation for delivering clinically relevant amount of drugs. Although a few limitations have to be overcome in the successful use of these non-polymer based DES, still these systems provide promising alternative approaches to currently available adverse reaction-inducing polymer coated DES. The goal of this study is to coat drug directly on metal surfaces without using any carriers and to release it for a period of time. In this way, once the drug is delivered, the underlying metal substrates may not create adverse responses. The tolerability of metals in coronary arteries with no serious adverse reactions has long been established [29–32].

Some therapeutic drugs naturally have strong adhesion towards certain material surfaces [33–36]. Paclitaxel (PAT) is one such drug which is also commonly used for treating in-stent restenosis [37]. PAT has been shown to strongly adsorb onto different materials including glass [35], polypropylene [35], silicones [35], and polytetrafluoroethylene [38]. In this study, we have explored the use of strong adhesion property of PAT to coat these molecules directly on Co–Cr alloy, a material which is used for making ultra-thin stent struts, and have investigated the *in vitro* drug release profiles of this system for up to 56 days.

2. Materials and methods

The Co–Cr–W–Ni alloy substrate (L605 grade) was purchased from High Tech Metals, Inc (Sylmar, CA). Absolute ethanol (200 proof), methylene chloride, acetone, and methanol were all purchased from Pharmo-AAPER (USA) and used as-received. Paclitaxel (>99% purity) was purchased from ChemieTek (Indianapolis, USA). HPLC-grade water, acetonitrile and methanol were purchased from Sigma-Aldrich (USA).

2.1. Preparation of cobalt–chromium alloy specimens

The Co–Cr alloy substrate was cut into 1 cm × 1 cm specimens. The specimens were cleaned by sonication in ethanol, acetone, and methanol twice for ten minutes each. Fresh solvents were used each time. The specimens were then dried using N_2 gas. Thus chemically cleaned Co–Cr alloy specimens are referred to here as control Co–Cr.

2.2. Direct coating of paclitaxel on Co–Cr alloy

A solution of paclitaxel was prepared in ethanol at a concentration of 1 mg/1 mL. A 25 μL aliquot of the prepared solution was placed on the surface of each chemically cleaned Co–Cr alloy specimen using a micropipette and the specimens were stored under ambient laboratory conditions. The ethanol was allowed to evaporate in air for 3 hours leaving behind a residue of paclitaxel on the alloy specimens. The specimens were then sonicated in 2 mL of ethanol for 1 minute to remove the weakly bound drug from the alloy surfaces, followed by air drying. Thus prepared paclitaxel coated alloy specimens are henceforth referred to here as Group-A. Another set of paclitaxel coated alloy specimens was prepared according to the method described above but were transferred to an oven for heat treatment before ethanol cleaning. The specimens were heated in air at 120 °C for 12 hours. The specimens were then cooled in ambient air for 1 hour before cleaning them in ethanol for 1 minute under sonication followed by air drying. Thus prepared specimens are referred to here as Group-B. The only difference between Group-A and Group-B was the introduction of heating step (in Group-B) before ethanol cleaning. Control specimens for both Groups-A and B were also prepared and are referred to here as Groups-C and D, respectively. For Groups C and D, the alloy specimens were subjected to drug deposition protocols described for Groups-A and B, respectively, but without employing the final ethanol cleaning procedure. A schematic of the preparation of specimens of Groups-A, B, C, and D are shown in Fig. 1. The description of specimens of Groups-A to D are provided in detail in Table 1.

2.3. Drug elution studies

Specimens (4 each) of Groups-A, B, C, and D were incubated in 2 mL of phosphate-buffered saline with 0.05% tween-20 (PBS/T-20) (pH = 7.4) at 37 °C. Tween-20 was added to increase the solubility of paclitaxel in PBS [39]. After respective time points (1, 3, 5, 7, 14, 28, and 56 days), the alloy specimens were taken out and immediately transferred to 2 mL of fresh PBS/T-20 solution. The PBS/T-20 samples collected at different time points were then analyzed for the quantity of drug released using HPLC. It is important to note that 1 mL of ethanol was added to PBS/T-20 sample containers (polypropylene tubes) and vigorously shaken before analyzing the samples in HPLC. This was done in order to avoid any potential drug loss to polypropylene container surfaces as reported in other studies [35]. Alcohol-based washing was previously used in the literature to extract the drug bound to the container surfaces [36]. Besides, the addition of ethanol further increases the solubility of paclitaxel in PBS/T-20, and improves accuracy for the quantification of drug eluted using HPLC.

2.3.1. High-performance liquid chromatography

The HPLC analysis was carried out using a Waters 2695 separations module with Waters 2487 Dual λ Absorbance Detector. A Nova-Pak® C18 column (3.9 mm × 150 mm; particle size – 4 μm; Part # WAT086344; Serial # 111937081140 77) was used. A mobile phase composition of water and acetonitrile (45:55 v/v) was used at a flow rate of 1.0 mL/min. A 10 μL volume of the sample was injected for analysis and chromatographic separations were carried out at 35 °C. The detector wavelength was fixed at 227 nm.

A standard stock solution of Paclitaxel was prepared in absolute ethanol (200 proof) at a concentration of 1 mg/mL. This solution was further diluted with ethanol and working solutions were prepared over a wide concentration range (1 ng/mL to 1099 ng/mL). Standard calibration curves were obtained for working solutions and the curves were linear over the ranges of 1–99 ng/mL and 99–1099 ng/mL with correlation coefficients of $R^2 = 0.9996$ and $R^2 = 0.9677$, respectively. The chromatographic data collected were analyzed using a Waters Millennium 32 software data system. The calibration graphs were constructed by plotting the concentration of paclitaxel (ng/mL) on the x-axis and the area of the peak (microvolts/sec) on the y-axis.

2.4. Surface characterization

Specimens of Groups-A, B, C, and D were characterized using X-ray photoelectron spectroscopy (XPS), scanning electron microscopy (SEM), and atomic force microscopy (AFM).

2.4.1. X-ray photoelectron spectroscopy

XPS measurements were performed on a Kratos Axis-Ultra instrument using a monochromatized Al Kα X-ray source ($E = 1486.7$ eV, 225 W), a hemispherical electron energy analyzer, and a channeltron detector array. Survey spectra were recorded with a pass energy of 160 eV while the high-resolution spectra were recorded with a pass energy of 20 eV (for O 1s and C 1s spectra) or 40 eV (for Co 2 p, Cr 2 p, W 4f, Ni 2 p, and N 1s spectra). All measurements were carried out using a nominal photoelectron takeoff angle of 90° with respect to the sample surface. The binding energy (BE) values for Co–Cr alloy specimens, before and after the coating of paclitaxel, were corrected by setting the standard hydrocarbon C 1s peak at 285 eV. The spectral deconvolution and peak area analysis were carried out using the Casa XPS software system to determine the elemental and component compositions. The reported BE values, atomic percentage compositions, and molar percentage concentrations of components represent the average of three distinct spots on each sample along with the corresponding standard deviations.

2.4.2. Scanning electron microscopy

A ZEISS EVO-40 (Germany) model SEM instrument was used in this study. The images were acquired using a working distance of 35–37 mm and an accelerating voltage of 5 kV. Prior to SEM imaging, the specimens were sputter coated with a thin layer of carbon.

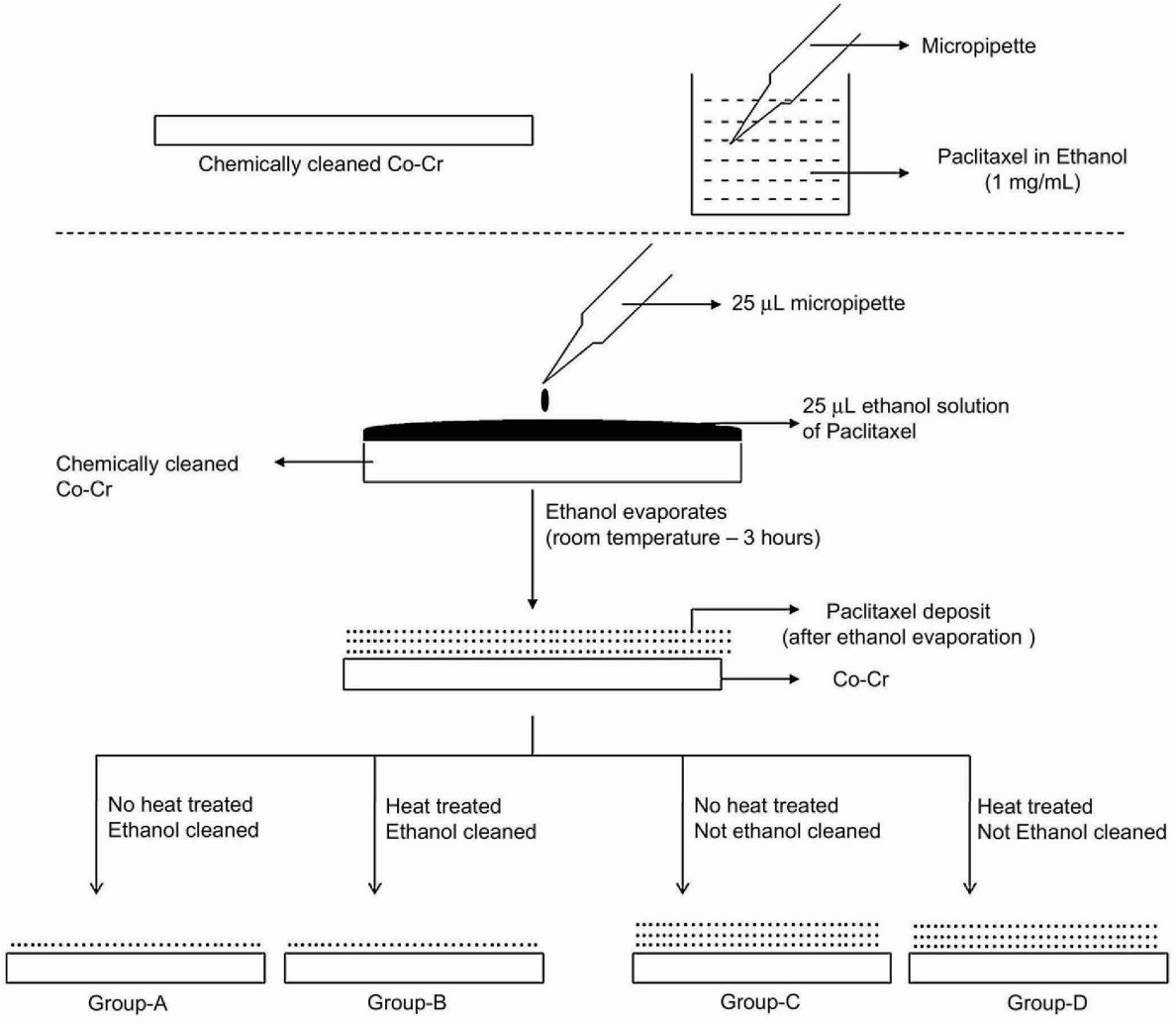

Fig. 1. Schematic of preparation of paclitaxel coated cobalt–chromium alloy specimens of Group-A, B, C, and D.

2.4.3. Atomic force microscopy

All AFM images were acquired with a Nanoscope III instrument (Digital Instruments, Inc. Santa Barbara, CA) at room temperature in air. The images were captured in tapping mode using Si_3N_4 cantilevers with a spring constant of 20–80 N/m. All the reported images were flattened using a third degree polynomial fit. The root-mean-square (RMS) roughness values were calculated from the average of at least four distinct spots (10 µm × 10 µm) on two different samples and reported here with their corresponding standard deviations.

Table 1
Descriptions of control Co–Cr and paclitaxel coated Co–Cr specimens of Groups-A, B, C, and D.

Sample Name	Description		
Control Co–Cr	Chemically cleaned cobalt–chromium alloy specimens		
Paclitaxel coated Co–Cr alloy			
Sample Name	Paclitaxel coated (25 µg/cm^2)	Heat treated (120 °C, 12 hours)	Ethanol cleaned
Group-A	Yes	No	Yes
Group-B	Yes	Yes	Yes
Group-C	Yes	No	No
Group-D	Yes	Yes	No

2.5. Statistical analysis

The experimental data collected are presented as the mean ± standard deviation. A one-way analysis of variance (ANOVA) was performed and statistical significance for difference was defined as $p < 0.05$.

3. Results

3.1. Delivery of paclitaxel from Co–Cr alloy

The initial drug loaded on Co–Cr alloy specimens of Groups A, B, C, and D was 25 µg/cm^2. After drug deposition, the specimens of Groups A and B were cleaned in ethanol to remove the weakly bound drug from the alloy surfaces. The ethanol solution used for cleaning was then analyzed in HPLC to calculate the amount of drug washed out during the cleaning protocols (Table 2). The difference between the initial drug loaded (25 µg) and the amount of drug washed out in ethanol provided the amount of drug that actually retained on the alloy surface after ethanol cleaning (or before immersion in PBS/T-20 media). Approximately, 20% and 25% of the initial drug loaded was retained on the alloy surfaces after ethanol

Table 2
Amount of drug retained on Co–Cr alloy specimens of Groups A and B after ethanol cleaning.

	Group – A	Group – B
Initial drug loaded	25 μg	25 μg
Amount of drug washed out in ethanol cleaning procedure	20.2 ± 0.7 μg	18.8 ± 0.3 μg
Total amount of drug retained on the alloy surface after ethanol cleaning (Initial drug loaded – Amount of drug washed out in ethanol)	4.8 ± 0.7 μg	6.2 ± 0.3 μg
Percentage of total amount of drug washed out in ethanol cleaning	81 ± 3%	75.1 ± 1.2%
Percentage of total amount of drug loaded on the alloy surface after ethanol cleaning	19 ± 3%	24.9 ± 1.2%

cleaning of specimens of Groups A and B, respectively. The amount of drug that was retained on the specimens of Group B was significantly ($p < 0.05$) greater than that of Group A. This suggests that the heating treatment improves the stability of paclitaxel on Co–Cr alloy surfaces.

Fig. 2a shows the drug release profiles of Groups A and B in PBS/T-20 solution. A sustained release profile was observed for both Groups A and B for up to 56 days. The total amount of drug released was statistically significant between all consecutive time points from day-1 to day-56 for both Groups A and B (Fig. 2a). Fig. 3a shows the actual amount of drug released between every two consecutive time points, and clearly demonstrates that paclitaxel was released from Co–Cr alloy surfaces in a sustained manner. The actual amount of drug released from specimens of Group B was significantly lower than that of the specimens of Group A on day-1 and between days-3 and 5 (Fig. 3a). This led to the release of less total drug from the specimens of Group B when compared to that of Group A for up to 7 days (Fig. 2a). No statistically significant difference in the total amount of drug released was observed between Groups A and B from day-14 to day-56. This suggests that a simple heating protocol provides improved stability of PAT on Co–Cr alloy surfaces. This effect is especially significant during the initial days of immersion in PBS/T-20, which cause PAT to be delivered from heated specimens (Group B) at a slower rate than unheated specimens (Group A). Fig. 2b shows the percentage of total drug release profiles for Groups A and B. Approximately, 7% and 5% of the total drug retained (after ethanol cleaning) was released from Groups A and B, respectively for up to 56 days. This suggests that PAT strongly adhered to Co–Cr alloy surfaces and only a limited amount of the total drug retained can be released for the time period investigated in this study.

Fig. 4a shows the drug release profiles of Groups C and D (PAT coated Co–Cr specimens which were not cleaned in ethanol) in PBS/T-20 solution. Burst release profiles were observed for both Groups C and D. No significant difference in the total amount of drug released was observed from day-1 to day-56. Approximately, 70–80% of the total drug loaded was released within day-1 and 90% of the total drug was released in 56 days. It is interesting to note that 10% of the total drug loaded was retained on the alloy surface even after 56 days. The percentage of drug retained on the surface was calculated based on the difference between the total drug loaded and the amount of drug released for up to 56 days. The actual amount of drug released between every two consecutive time points of specimens of Groups C and D are shown in Fig. 4b. A significant amount of drug was burst released within the first 3 days followed by a slow and sustained release for up to 56 days. Interestingly, the actual amounts of drug released from the specimens of Groups C and D after 7 days are in the same range as the amount of drug released from Groups A and B (4–8 nanograms/day).

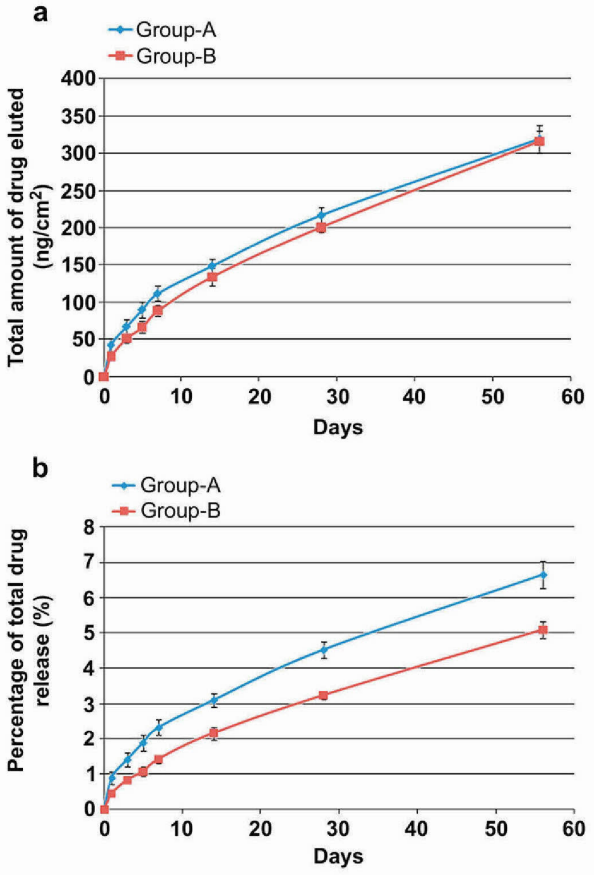

Fig. 2. (a) *In vitro* drug release profiles of specimens of Groups A and B; (b) Percentage of total drug release profiles of specimens of Groups A and B.

This suggests that once the loosely bound PAT is removed by solvent cleaning (as in Groups A and B) or burst released (as in Groups C and D), the remaining strongly bound PAT molecules will be slowly released over a period of time.

The control Co–Cr alloy and four groups (A, B, C, and D) of drug coated specimens were thoroughly characterized using SEM, AFM, and XPS to study the morphology, distribution, and attachment of PAT on Co–Cr alloy specimens.

3.2. SEM characterization

Fig. 5a–f shows the SEM images of control Co–Cr alloy and PAT coated Co–Cr alloy specimens. A flat surface was observed for control Co–Cr alloy with few surface pits. Two different forms of paclitaxel crystals, spheres (Fig. 5b and e) and needles (Fig. 5c), were formed on the specimens of Groups C and D. The SEM images are particularly useful in determining the shape and distribution of aggregates of PAT molecules (crystals) on the specimens of Groups C and D (Fig. 5b, c, and e). However, the resolution of SEM limited imaging the molecular distribution of PAT molecules on the specimens (Fig. 5d and f).

3.3. AFM characterization

The AFM tapping mode height and amplitude images of control and PAT coated Co–Cr alloy specimens are shown in Fig. 6a–j. The

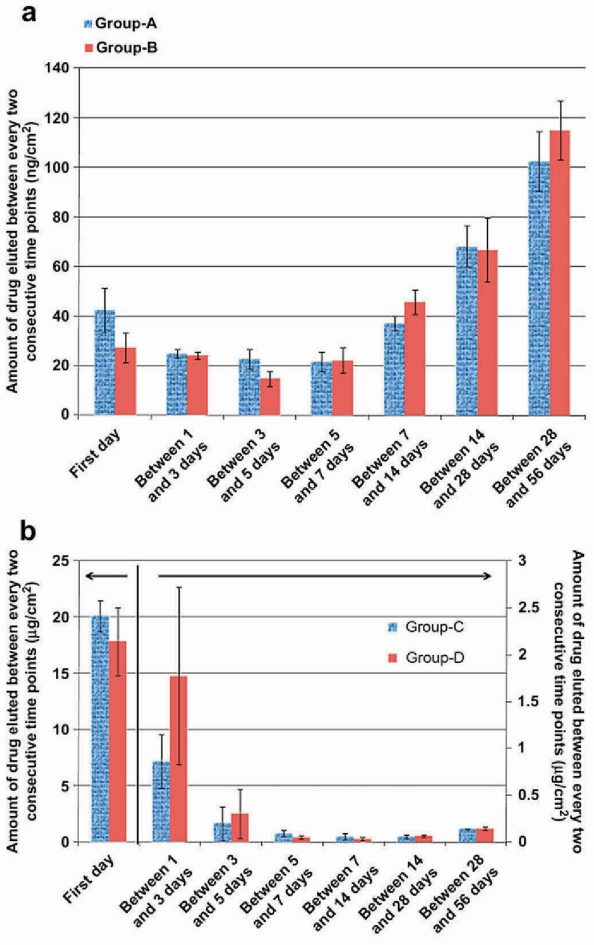

Fig. 3. Amount of drug eluted between every two consecutive time points of Groups A and B (a) and Groups C and D (b).

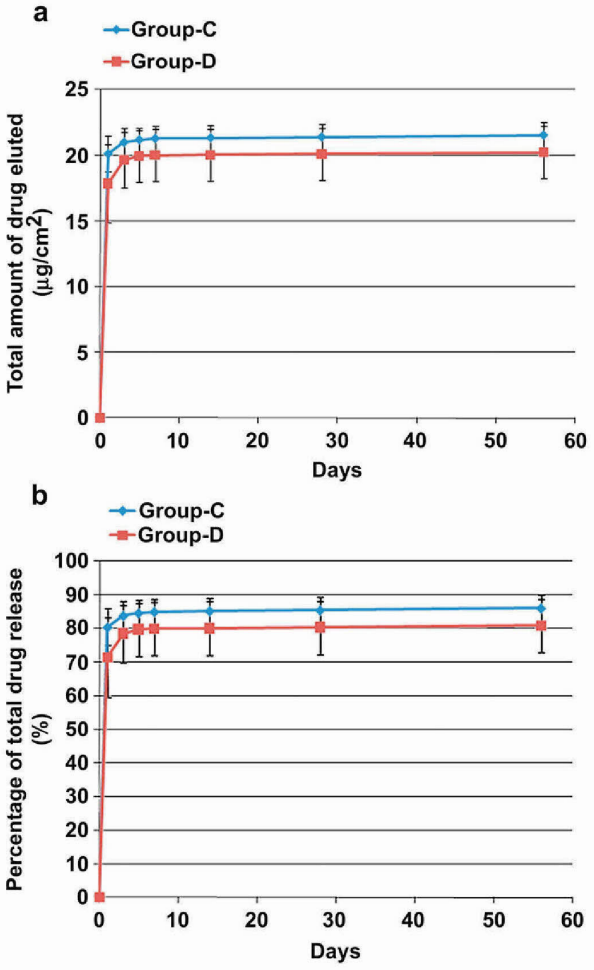

Fig. 4. (a) *In vitro* drug release profiles of specimens of Groups C and D; (b) Percentage of total drug release profiles of Group C and D.

control Co–Cr showed flat topography with few pits and surface defects (Fig. 6a and b). The RMS roughness value of control Co–Cr was 19.6 ± 7.3 nm. The formation of sphere and needle shaped PAT crystals on Co–Cr was clearly observed in Groups C and D (Fig. 6c, d, g, and h). The RMS roughness values of the specimens of Groups C and D were 282.3 ± 52.7 nm and 148.6 ± 45.7 nm, respectively. This significant increase in surface roughness values demonstrated the presence of drug aggregates on Co–Cr alloy. These results are qualitatively consistent with SEM images. AFM images were also useful in observing the molecular distribution of PAT on the specimens of Groups A and B (Fig. 6e, f, i, and j). The RMS roughness values of the specimens of Groups A and B were 24.0 ± 12.2 nm and 16.2 ± 5.8 nm, respectively.

3.4. XPS characterization

The high resolution XPS C 1s, O 1s, N 1s, Co 2p, Cr 2p, W 4f, and Ni 2p spectra were collected before and after the deposition of PAT on Co–Cr alloys. The chemical compositions of control Co–Cr alloy and PAT coated Co–Cr alloys (Groups A and C) are shown in Fig. 7a. When compared to control Co–Cr, the specimens of Group C showed a significant increase in the concentration of carbon and a significant decrease in the concentrations of oxygen, and other elements (Co, Cr, W, and Ni) specific to the alloy substrate. Since the PAT contains 47 carbon atoms, the concentration of carbon is expected to increase after the drug deposition. Also, when the drug is deposited on the alloy, the concentrations of oxygen (the main element in the surface oxides of Co–Cr alloy) and other elements in the alloy substrate are expected to decrease due to attenuation of XPS signals. Such increases in the concentration of carbon and decreases in the concentrations of oxygen and other elements are less in Group A when compared to Group C. However, it is imperative to note that the concentration of carbon in Group A is significantly greater than that of control Co–Cr and the decrease in the concentrations of oxygen and other elements is significantly lower than that of control Co–Cr. This strongly suggests that after ethanol cleaning, some PAT molecules are still strongly adsorbed onto Co–Cr alloy surfaces. Similar results were also observed for specimens of Groups D and B (Fig. 7b).

Besides the unavoidable carbon contaminant, a trace of nitrogen contaminant was also observed on control Co–Cr. Similar contamination was reported by several other research groups for metal oxide samples [40,41]. A ratio of carbon to elements in the underlying metal substrate has been used in the literature to precisely determine the adsorption/desorption of organic molecules on metal substrates

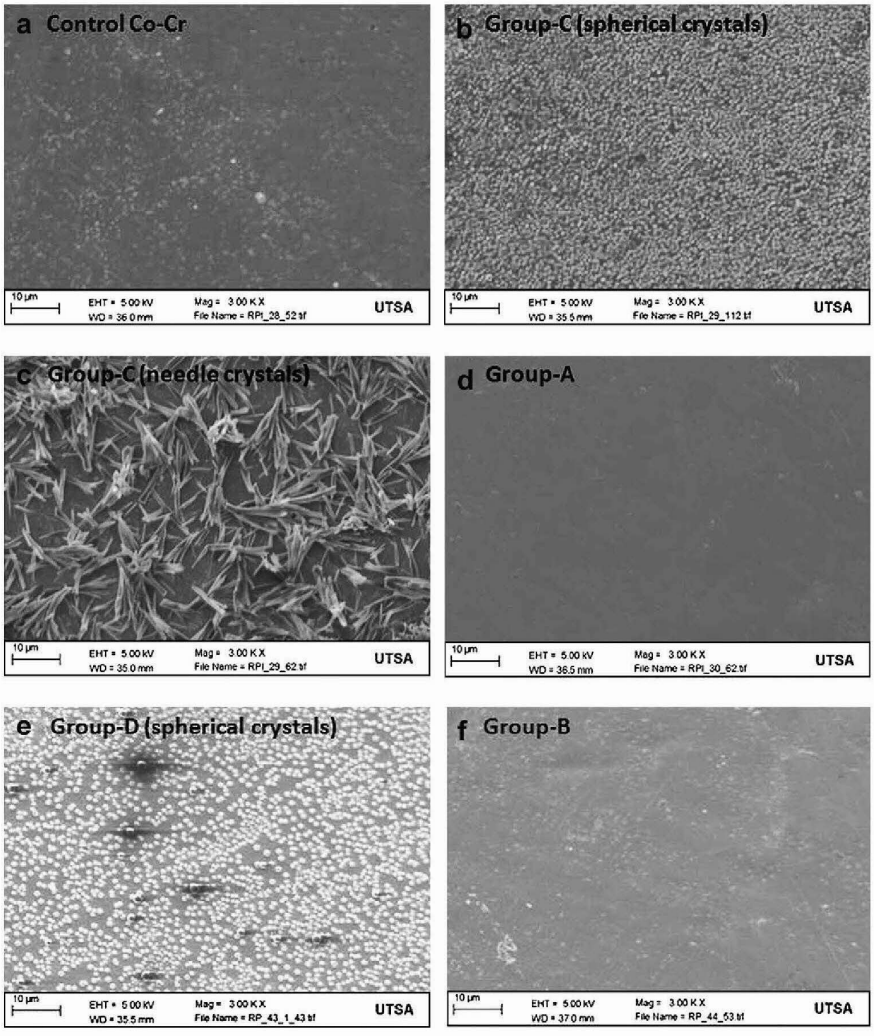

Fig. 5. SEM images of control Co–Cr alloy (a); group-C (spherical crystals) (b); group-C (needle crystals) (c); group-A (d); group-D (spherical crystals) (e); group-B (f).

[42–45]. We used such an approach to determine the adsorption of PAT on Co–Cr alloys. Since ample amount of carbon and oxygen atoms are present in paclitaxel, the ratios of the concentration of these elements to the concentrations of cobalt, chromium, tungsten, and nickel were calculated to qualitatively determine the presence of PAT on Co–Cr alloys. A ratio of carbon to oxygen was also calculated for all the specimens. Fig. 8a shows C/[Co + Cr + W + Ni], O/[Co + Cr + W + Ni], and C/O ratios of control Co–Cr and Groups A and C. All the three ratios calculated for Group A were greater than that of control and lower than that of Group C. This further confirms the presence of strongly bound PAT molecules on Co–Cr alloy after ethanol cleaning. As expected, the ratios were highest for Group C due to the presence of aggregates of drug. Similar results were also observed for the specimens of Groups B and D (Fig. 8b).

The high resolution XPS C 1s spectrum of control Co–Cr alloy was deconvoluted into three components: the peaks at 285 eV, 286.1 eV, and 288.6 eV were assigned to C–C, C–O, and C=O bonds of hydrocarbon contaminants (Fig. 9a and Table 3a). Several studies in the literature have reported the adsorption of such contaminants on metal oxide surfaces [45,46]. Also, the C 1s peak of hydrocarbon contamination is commonly used as an internal standard for instrument calibration [46]. The C 1s spectrum of paclitaxel (in powder form) was deconvoluted into four components: the peaks of the components at 285 eV, 286.6 eV, 289.2 eV, and 291.6 eV were assigned to carbon atoms in hydrocarbon, hydroxyl, ester, and aromatic ring groups of PAT (Fig. 9b and Table 3a). The C 1s spectra of Groups C and D were deconvoluted into four components: the peaks of the components, C 1s (1), C 1s (2), C 1s (3), and C 1s (4) were observed at 285 eV, between 286.4 and 286.9, between 288.4 and 288.9, and between 290.4 and 291.2 eV, respectively. C 1s (1) was assigned to C–C bonds of PAT; C 1s (2) was assigned to C–OH bonds of PAT; C 1s (3) was assigned to O=C–O bonds of PAT; and C 1s (4) was assigned to $\pi \rightarrow \pi^*$ shake-up satellite from the aromatic rings of PAT. Thus, the C 1s components of Groups C and D are in excellent agreement with the C 1s components of PAT powder. For Groups A and B, the components C 1s (1), C 1s (2), and C 1s (3) observed were similar to that of Groups C and D. However, the C 1s (4) component was missing in both Groups A and B (Fig. 9a and Table 3a). This could be due to the lesser amount of drug present on these specimens [22].

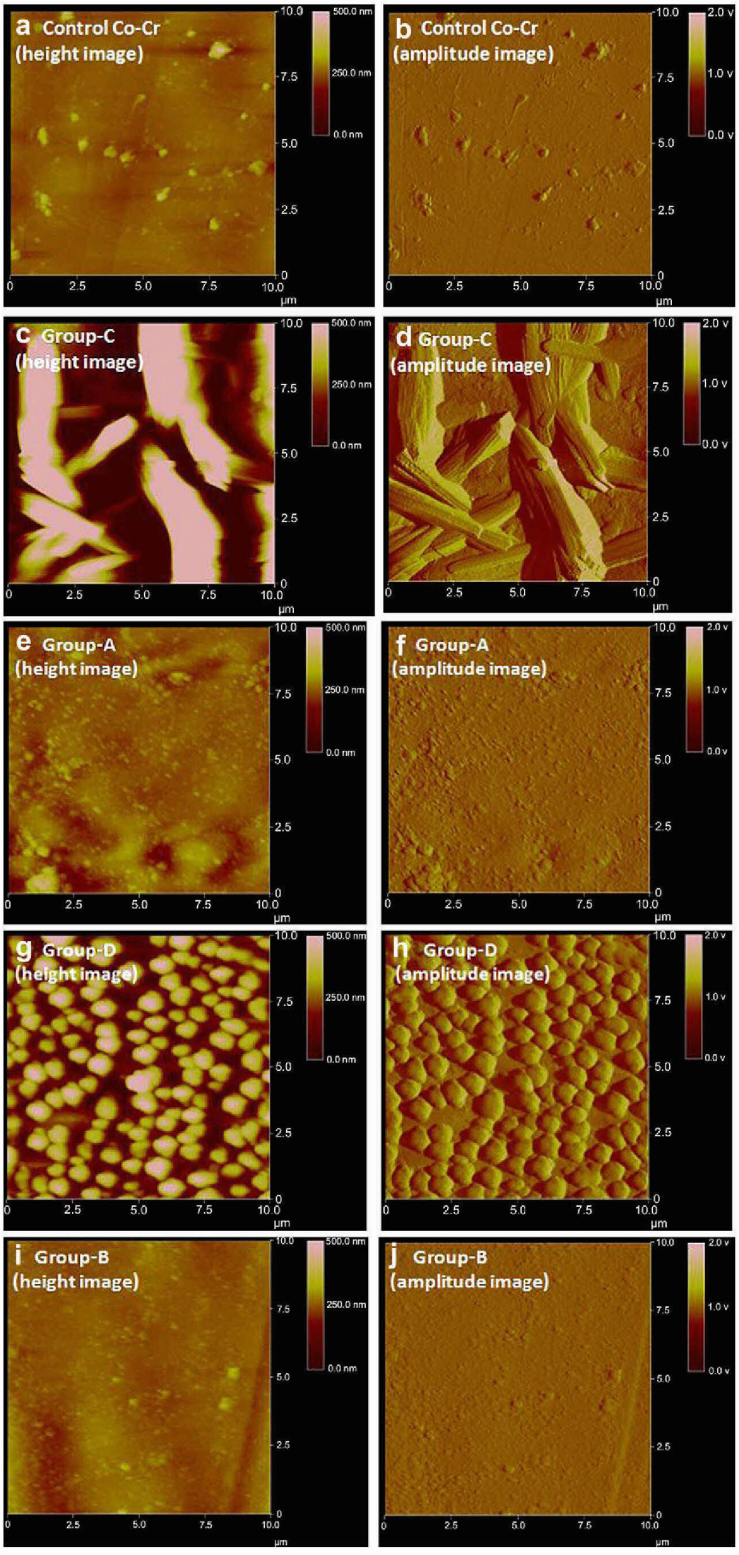

Fig. 6. AFM images of control Co–Cr (a,b), Group-C (c,d), Group-A (e,f), Group-D (g,h), and Group-B (i,j).

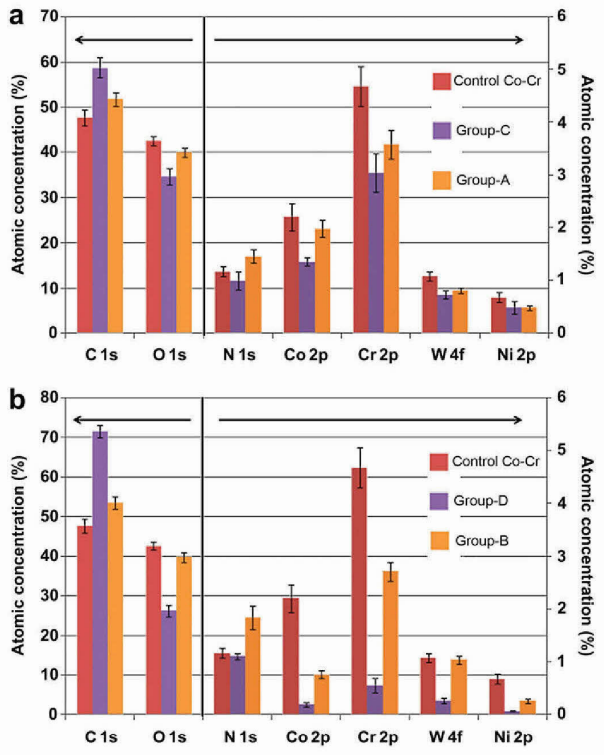

Fig. 7. XPS determined atomic compositions of control, Groups C and A specimens (a), and control, Groups D and B specimens (b).

The O 1s XPS spectrum of control Co–Cr was deconvoluted into three components: the peaks of the components, O 1s (1) at 529.9 eV, O 1s (2) at 531.6 eV, and O 1s (3) at 533.4 eV were assigned to metal oxide (O_2^-) species, hydroxide (OH^-) species, and H_2O species, respectively (Fig. 9c and Table 3b). The O 1s spectrum of PAT (in powder form) was deconvoluted into two components: the peaks of the components at 532.4 eV and 533.6 eV were assigned to oxygen atoms in O–C and O–C=O bonds, respectively (Fig. 9d and Table 3b). The O 1s spectra of Groups A, B, C, and D were all deconvoluted into three components: the peaks of the components, O 1s (1), O 1s (2), and O 1s (3) were observed between 529.9 and 530.1, between 531.5 and 532.2, between 533 and 534.3 eV, respectively (Fig. 9c and Table 3b). O 1s (1) was assigned to metal oxide species; O 1s (2) was assigned to O–C bonds of PAT; O 1s (3) was assigned to O–C=O bonds of PAT. The O 1s components of Groups A, B, C, and D are in good agreement with the O 1s components of PAT powder. These results suggest that PAT molecules were bound to Co–Cr alloy surfaces.

4. Discussion

Most currently available drug-eluting stents (DES) in the market use polymer-based carriers for delivering drugs. However, there are a number of safety issues associated with polymer-based DES: (a) the polymers cause adverse responses including inflammatory and hypersensitive (allergic) reactions [10–14,47]; (b) mechanical defects such as cracks, fissures, peeling of polymer layers from the stent, roughened surface with irregularities, and waviness have been observed in the polymer coatings of commercially available DES after balloon catheter expansion [48] and such defects can increase the risk of thrombosis; and (c) delayed and incomplete endothelialization is frequently observed [9,47,49]. Hence, there is a need to deliver drugs from stents without using polymer carriers. In this study, PAT was directly coated on Co–Cr alloy surfaces using its own strong adhesion property and the *in vitro* drug release profiles of this system were investigated.

Paclitaxel has strong binding properties towards different material substrates such as glass, polypropylene, and silicone [35]. Song et al. [35] examined the binding of PAT to glass and plastic containers in aqueous solution and tissue culture medium. PAT was more strongly adsorbed on to glass than plastic containers. Several other studies have also reported the adsorption of PAT on various plastic container surfaces during *in vitro* drug elution studies. Palmgren et al. [36] investigated the adsorption of various other drugs on plastic containers in deionized water and buffer solution. Acidic drugs such as hydrochlorothiazide, naproxen, probenicid, and indomethacin showed no adsorption on plastic containers in either water or buffer solution. However, basic drugs such as metoprolol, medetomidine, propranolol, and midazolam strongly adsorbed on polystyrene tubes especially when the storage

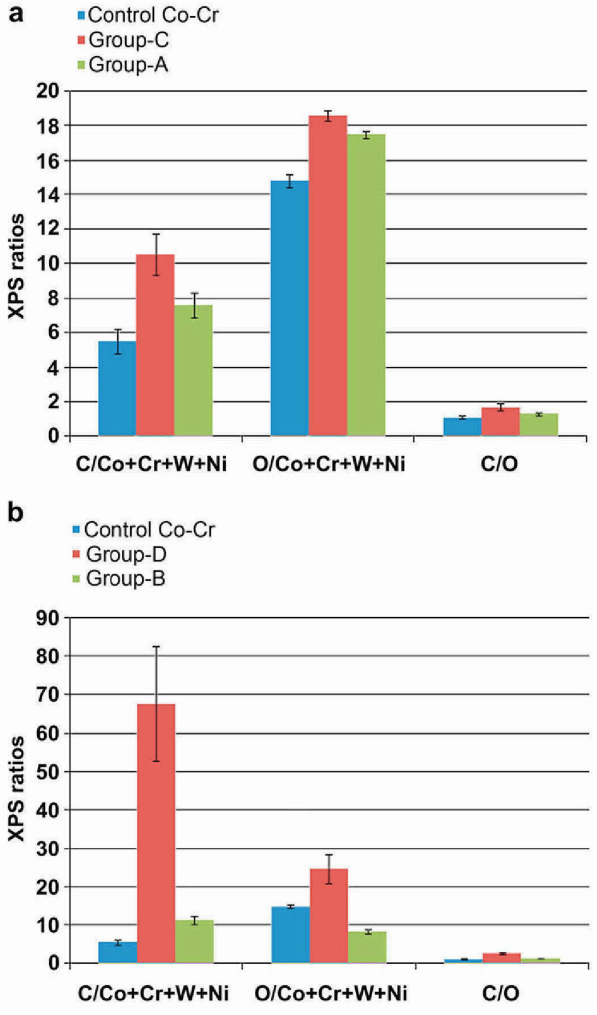

Fig. 8. XPS determined C/Co + Cr + W + Ni, O/Co + Cr + W + Ni, and C/O ratios of control, Groups C and A (a), and Groups D and B (b).

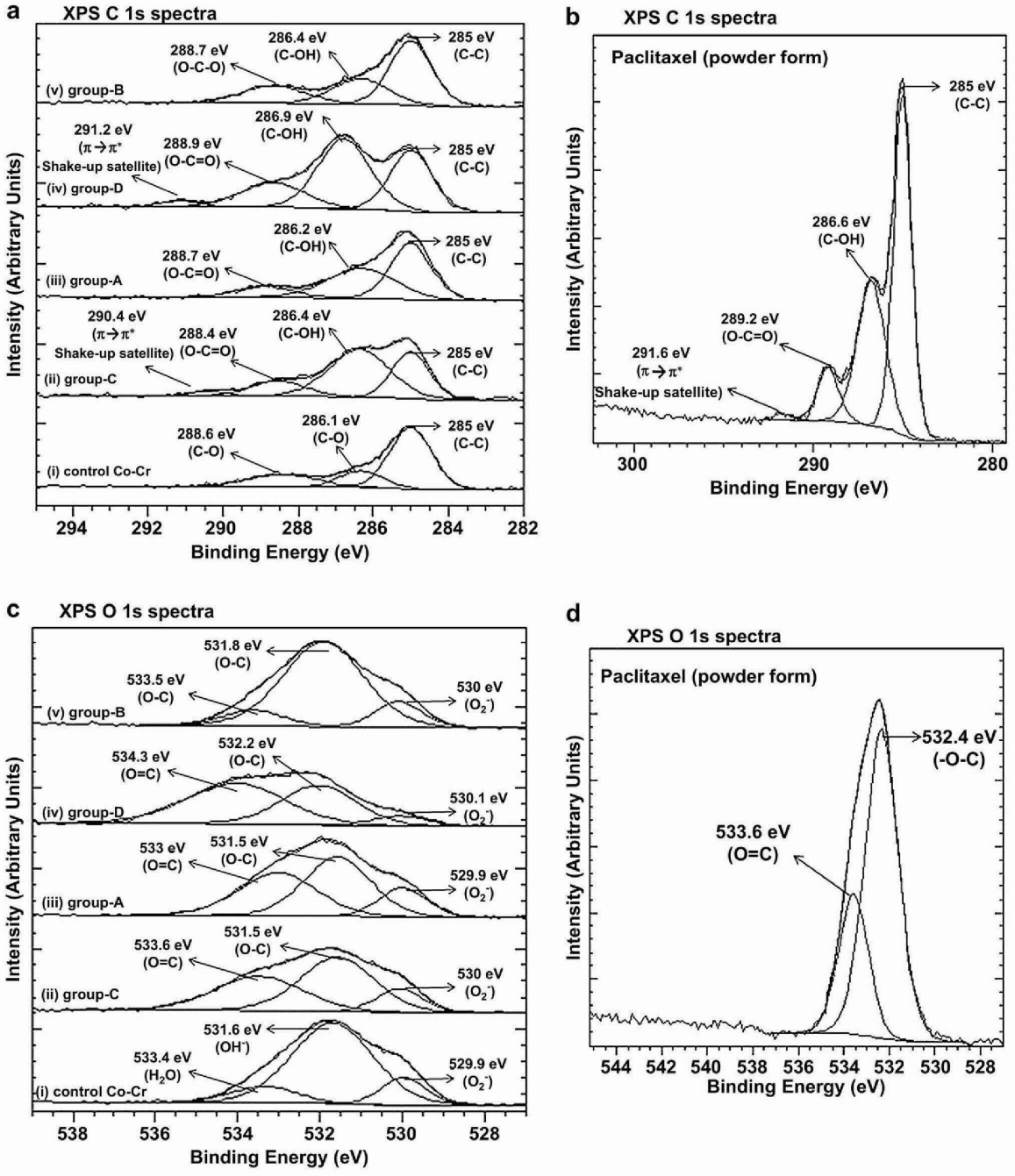

Fig. 9. XPS C 1s spectra of control Co–Cr and groups-A to D (a); C 1s spectrum of paclitaxel (powder form) (b); O 1s spectra of control Co–Cr alloy and groups-A to D (c); and O 1s spectra of paclitaxel (powder form) (d).

medium was water. No loss of drug has been observed in buffer solution and this could be attributed to buffer ions' competition for plastic surfaces which could prevent drug interactions. These studies suggested that the adsorption of drug on a material surface depends on several factors: (a) chemical nature of the drug; (b) physiochemical properties of the material surface; and (c) solvent-drug properties. The storage temperature and drug concentration also play a critical role in determining the adsorption properties of a drug [50]. To the best of our knowledge, no reports have been published on the mechanism of PAT adsorption to various material surfaces.

The hypothesis for the direct attachment of PAT on Co–Cr alloy is that the drug forms extensive hydrogen bonding with metal oxide surfaces, which have plenty of hydroxyl groups as inferred

from the XPS O 1s spectra (75% of oxygen atoms present on Co–Cr alloy surface belong to hydroxyl groups – Table 3b). The PAT molecules interact with each other through hydrogen bonding [51]. When the ethanol is allowed to evaporate after drug loading on the alloy surfaces, the intermolecular hydrogen bonding of PAT molecules drive them to form aggregates of crystals [52] (as in Groups C and D). However, the specimens coated with aggregates of PAT crystals showed burst release in PBS/T-20 (during drug elution studies) or ethanol (during ethanol cleaning procedure). This could be due to the reason that ion species in PBS/T-20 might interfere with intermolecular hydrogen bonding of PAT molecules [53] in the aggregates and result in the release of drug crystals. Organic solvents such as ethanol form hydrogen bonding with PAT molecules and this could have caused the loss of integrity of aggregates of PAT. However, it is interesting to observe that neither ions in PBS/T-20 nor ethanol molecules could remove all the PAT molecules that are strongly adhered to Co–Cr alloy surfaces. This is clearly evident from the specimens of Groups A and B, which showed a sustained release of the retained drug after the removal of drug crystals during ethanol cleaning. Similar effect was also seen in Groups C and D, when most of the drug crystals were released during the first 3 days of PBS/T-20 immersion, the remaining drug retained on the surface was eluted at a sustained rate for a period of 56 days. These behaviors could be due to extensive hydrogen bonding interactions between PAT molecules and high density surface hydroxyl groups of metal oxide. Based on this discussion, we hypothesize that PAT forms a molecular coating (strongly bound) on Co–Cr alloy surface and crystals of drug (weakly bound) on top of the strongly bound molecular layer (Fig. 10a). The weakly bound crystals release quickly and cause the burst effect in elution profiles (Fig. 10b), while the strongly bound molecules release at a sustained rate (Fig. 10c).

The unpolished chemically cleaned Co–Cr alloy specimens were used in this study to investigate the direct coating and delivery of paclitaxel. However, most commercially available drug-eluting stents have been primarily finished by electropolishing and acid passivation. Electropolishing typically replaces native surface oxide with more compact and smoother oxide [54]. However, the oxide layer in both native unpolished and electropolished Co–Cr alloy specimens is primarily composed of elements such as chromium, cobalt, and oxygen [45,55–57]. Besides, the metal oxides in both the cases are typically enriched with surface hydroxyl groups [45,55–57]. Since we assume that the bonding of paclitaxel to alloy surfaces mainly occurs through hydroxyl groups of the oxide layer, the chemical and physical differences of unpolished versus electropolished surfaces may not have a significant impact on the adhesion of paclitaxel.

Heat treatment has been previously used in the literature to improve the stability of organic molecules on metal oxide surfaces [58,59]. Gawalt et al. [58] has showed that organic molecules such as alkanephosphonic acids can be self-assembled on the native oxide surface of titanium. However, these molecules have shown poor stability and can easily be removed during solvent rinsing. A gentle heat treatment at 120 °C for 18 hours following organic coating deposition has tremendously improved the stability of these molecules on titanium. These strongly bound molecules are then highly resistant to solvent washing or mechanical peel testing. This study suggested that hydrogen bonding interactions between phosphonic acid groups and metal surface oxide play a critical role in the coating of these molecules on titanium and the bonding interactions are further strengthened by the heating phenomenon [58]. In our study, the amount of drug released from the specimens of Group-B (heat treated) was significantly lower than that of Group-A (unheated) during the initial 7 days. However, no significant difference in the amount of drug released was observed between these two groups after 7 days and for up to 56 days. This suggests that the heat treatment provides enhanced stability to strongly bound PAT molecules on Co–Cr alloy surfaces especially during the initial days of PBS/T-20 immersion. No significant difference in the amount of drug released was observed between

Table 3a
XPS determined C 1s components of control and PAT coated Co–Cr alloy specimens.

Sample	Control Co–Cr alloy			
Components	C 1s (1)	C 1s (2)	C 1s (3)	C 1s (4)
BE (eV)	285	286.1 ± 0.2	288.6 ± 0.2	
Atomic conc. (%)	49.8 ± 10.6	32.2 ± 13.2	18.0 ± 2.9	
Sample	Paclitaxel (powder form)			
Components	C 1s (1)	C 1s (2)	C 1s (3)	C 1s (4)
BE (eV)	285	286.6 ± 0.1	289.2	291.6 ± 0.1
Atomic conc. (%)	58.7 ± 4.5	32.7 ± 2.7	8.1 ± 1.5	0.6 ± 0.3
Sample	Group-C (Co–Cr/PAT, unheated and not cleaned in ethanol)			
Components	C 1s (1)	C 1s (2)	C 1s (3)	C 1s (4)
BE (eV)	285	286.4 ± 0.1	288.4 ± 0.1	290.4 ± 0.1
Atomic conc. (%)	31.3 ± 2.8	48.7 ± 2.8	17.1 ± 2.2	2.9 ± 0.9
Sample	Group-A (Co–Cr/PAT, unheated and cleaned in ethanol)			
Components	C 1s (1)	C 1s (2)	C 1s (3)	C 1s (4)
BE (eV)	285	286.2 ± 0.2	288.7 ± 0.2	
Atomic conc. (%)	42.8 ± 8.1	39.2 ± 9.1	18.0 ± 5.5	
Sample	Group-D (Co–Cr/PAT, heated and not cleaned in ethanol)			
Components	C 1s (1)	C 1s (2)	C 1s (3)	C 1s (4)
BE (eV)	285	286.9 ± 0.2	288.9 ± 0.3	291.2 ± 0.1
Atomic conc. (%)	29.2 ± 5.0	52.5 ± 7.3	14.6 ± 4.1	3.6 ± 1.3
Sample	Group-B (Co–Cr/PAT, heated and cleaned in ethanol)			
Components	C 1s (1)	C 1s (2)	C 1s (3)	C 1s (4)
BE (eV)	285	286.4 ± 0.1	288.7 ± 0.1	
Atomic conc. (%)	52.3 ± 5.6	28.4 ± 6.3	19.3 ± 1.5	

Table 3b
XPS determined O 1s components of control and PAT coated Co–Cr alloy specimens.

Sample	Control Co–Cr alloy		
Components	O 1s (1)	O 1s (2)	O 1s (3)
BE (eV)	529.9	531.6	533.4 ± 0.1
Atomic conc. (%)	13.6 ± 1.5	74.3 ± 6.2	12.1 ± 4.7
Sample	Paclitaxel (powder form)		
Components	O 1s (1)	O 1s (2)	O 1s (3)
BE (eV)	–	532.4 ± 0.1	533.6 ± 0.1
Atomic conc. (%)	–	62.2 ⊥ 13.8	37.8 ⊥ 13.8
Sample	Group-C (Co–Cr/PAT, unheated and not cleaned in ethanol)		
Components	O 1s (1)	O 1s (2)	O 1s (3)
BE (eV)	530	531.5	533.6 ± 0.1
Atomic conc. (%)	14.1 ± 1.8	45.7 ± 4.1	40.2 ± 4.9
Sample	Group-A (Co–Cr/PAT, unheated and cleaned in ethanol)		
Components	O 1s (1)	O 1s (2)	O 1s (3)
BE (eV)	529.9 ± 0.1	531.5 ± 0.1	533
Atomic conc. (%)	12.7 ± 3.9	50.2 ± 8.4	37 ± 4.8
Sample	Group-D (Co–Cr/PAT, heated and not cleaned in ethanol)		
Components	O 1s (1)	O 1s (2)	O 1s (3)
BE (eV)	530.1 ± 0.1	532.2 ± 0.1	534.3 ± 0.4
Atomic conc. (%)	6.1 ± 1.5	44.2 ± 4.0	49.7 ± 3.4
Sample	Group-B (Co–Cr/PAT, heated and cleaned in ethanol)		
Components	O 1s (1)	O 1s (2)	O 1s (3)
BE (eV)	530	531.8 ± 0.1	533.5 ± 0.1
Atomic conc. (%)	14 ± 1.1	73.7 ± 2.7	12.3 ± 1.9

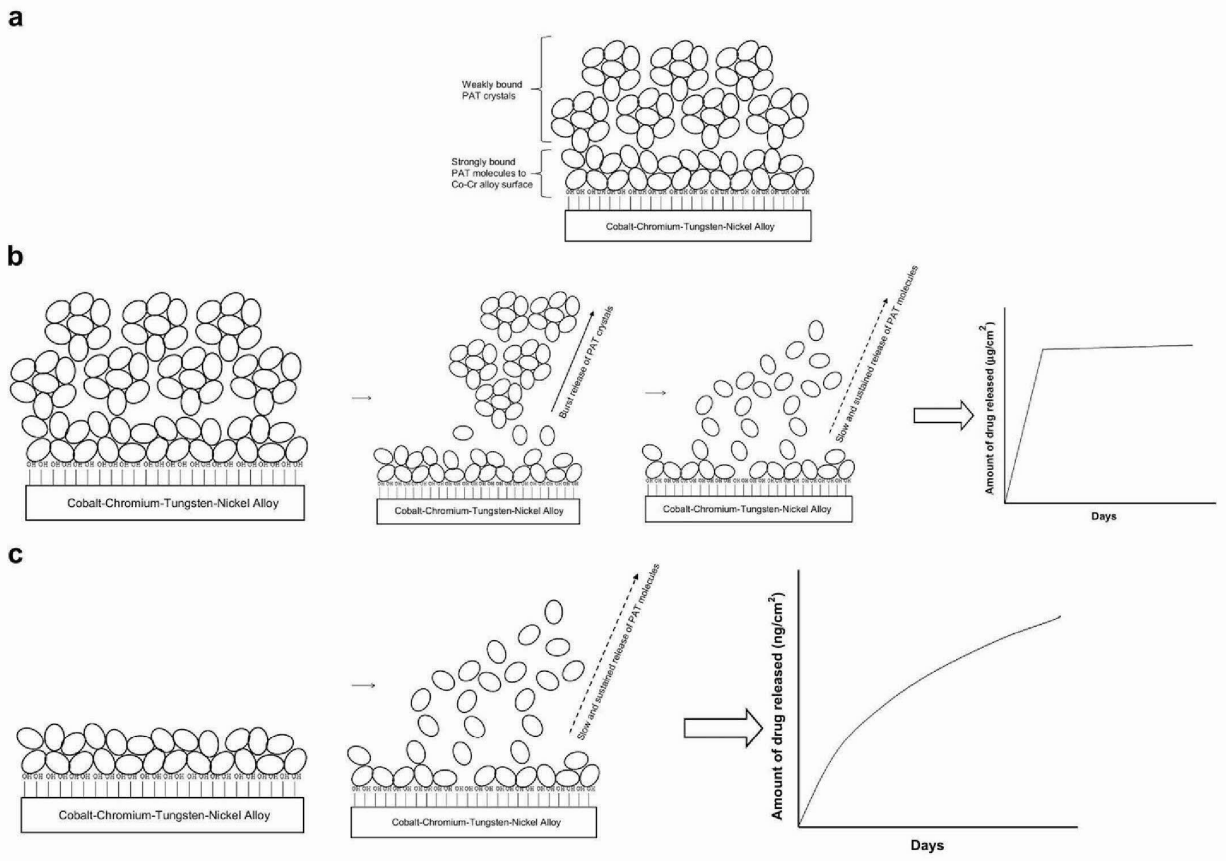

Fig. 10. (a) Schematic of the formation of PAT coating on Co–Cr alloy, (b) Schematic of the drug release from Groups C and D – Initial burst release of PAT crystals followed by a slow and sustained release of PAT molecules, (c) Schematic of the drug release from Groups A and B – Slow and sustained release of PAT molecules.

the Groups-C and D, which suggests that the heat treatment does not have a significant effect in controlling the burst release of weakly bound PAT crystals. The physicochemical properties of PAT have been well studied [60]. Liggins et al. [60] investigated the thermal stability of paclitaxel using differential scanning calorimetry (DSC) and thermogravimetric analysis (TGA). The degradation of PAT was observed at ~248 °C. DSC showed no transitions of PAT before the drug melted at 220 °C while no weight loss was observed by TGA. Hence, the temperature of 120 °C used in this study to heat treat the specimens would not affect the physicochemical properties of PAT.

The solid state form (crystalline or amorphous) of the drug is crucial in determining its solubility, stability, and bioavailability [61,62]. The amorphous form of the drug typically shows greater solubility than its crystalline form [61,62]. This is due to the fact that the molecules are randomly placed in amorphous form while the molecules are arranged in regular array in crystalline form [61]. Hence, the bioavailability, which in turn decides the therapeutic effect of drug, is greater for amorphous form when compared to crystalline form [62]. However, amorphous forms are thermodynamically metastable and can convert into crystalline form [61]. Hence, different techniques have been developed in the literature for maintaining drugs in amorphous form [62]. In this study, the coating of PAT on Co–Cr alloy resulted in the formation of both weakly bound crystals and strongly bound molecules. If a technique is developed to reduce the formation of PAT crystals on Co–Cr, it could increase the amount of strongly bound PAT molecules on the alloy surfaces. This might play a significant role in preventing burst releases in Groups C and D (and during the ethanol wash in Groups A and B).

Lee et al. [38] has investigated the delivery of PAT directly from polytetrafluoroethylene (PTFE)-based haemodialysis grafts. A burst release of PAT was followed by a slower and sustained release for up to 8 weeks. In addition, more than 50% of the initial drug loaded remained on the surface even after 8 weeks. Our results are in excellent agreement with this study that PAT shows a sustained release after an initial burst; and a portion of the drug remains on the material surface even after 2 months of immersion in buffered saline solution. Lee et al. [38] have proposed that the PAT adheres onto numerous surface pits of the rough PTFE surface and releases at a sustained rate. Another study has also explored the possibility of coating PAT directly on to drug-eluting balloon catheters by roughening the surface [63]. These studies in general have shown that surface roughness of a material has a critical role in delivering drugs at a sustained rate. Some other studies have also investigated the delivery of paclitaxel directly from stainless steel surfaces [64,65]; however, no mechanisms on drug adsorption and delivery have been reported.

The proposed mechanism for PAT release from Co–Cr alloy surface is the breakage of hydrogen bonds between PAT molecules and metal oxide surfaces by ions in the PBS/T-20 solution. The phosphate ions in PBS/T-20 have strong affinity towards metal oxide surfaces. On the other hand, PAT is hydrophobic drug and it might prefer to adsorb to metal surfaces rather than remain soluble

in water. Hence, a competition between these events may allow the drug to be delivered at a sustained rate. Also, we do not eliminate the roles of pits and surface defects of Co–Cr alloy surfaces in delivering drugs at a sustained rate.

The amount of PAT actually coated on the alloy surfaces after ethanol wash (Groups A and B) was ~5 μg/cm^2 (Table 2). This is less than the amount of PAT that is coated on the commercially available polymer coated TAXUS drug-eluting system (100 μg/cm^2) [39]. The possibility to increase the amount of strongly bound PAT molecules directly on Co–Cr alloy surfaces are currently under investigation. The use of nanostructured Co–Cr alloy surfaces with increased surface area will be explored for this purpose [66]. Also, the required dose of drug to prevent restenosis using non-polymer based DES may be smaller than that of polymer-based DES because of the following reasons: (a) no polymer-induced restenosis in non-polymer based DES; (b) the drug coated will be in direct contact with the arterial wall, hence the possibility of delivered drug to reach the targeted site is higher.

5. Conclusions

The natural strong adhesion property of paclitaxel was used in this study to attach these molecules directly to cobalt–chromium alloy surfaces. *In vitro* drug release profiles of this system were investigated for up to 56 days. Paclitaxel was directly coated on Co–Cr alloy surfaces and four different groups of specimens were prepared using the following two variables: (a) ethanol cleaning after drug deposition; and (b) heat treatment after drug deposition. The drug coated specimens which were cleaned in ethanol showed sustained release profiles. The specimens which were not cleaned in ethanol showed burst release profiles. The ethanol removes loosely bound drug crystals from the alloy surfaces and leaves behind strongly bound molecules which then release at a sustained rate. Heat treatment of the metal after drug coating improves the stability of PAT on Co–Cr alloy and allows the drug to be delivered at a slower rate than unheated specimens especially during the initial 7 days. SEM and AFM showed the formation of two different types of PAT crystals, spheres and needles, on Co–Cr alloy surfaces before ethanol cleaning. After ethanol cleaning, AFM showed the molecular distribution of PAT on Co–Cr alloy. XPS confirmed the attachment of PAT on all four different groups of specimens. Thus, this study demonstrated that PAT can be coated and released from Co–Cr alloy surfaces without using carriers.

Appendix

Figures with essential colour discrimination. Many of the figures in this article have parts that may be difficult to interpret in black and white. The full colour images can be found in the on-line version, at doi:10.1016/j.biomaterials.2010.03.043.

References

[1] Grundy SM. Atlas of atherosclerosis: risk factors and treatment. 4th ed. Philadelphia: Current Medicine Group; 2005.
[2] Serruys PW, Jaegere PD, Kiemeneij F, Macaya C, Rutsch W, Heyndrickx G, et al. A comparison of balloon-expandable-stent implantation with balloon angioplasty in patients with coronary artery disease. N Engl J Med 1994;331(8):489–95.
[3] Fischman DL, Leon MB, Baim DS, Schatz RA, Savage MP, Penn I, et al. A randomized comparison of coronary-stent placement and balloon angioplasty in the treatment of coronary artery disease. N Engl J Med 1994;331(8):496–501.
[4] Kipshidze N, Dangas G, Tsapenko M, Moses J, Leon MB, Kutryk M, et al. Role of the endothelium in modulating neointimal formation: vasculoprotective approaches to attenuate restenosis after percutaneous coronary interventions. J Am Coll Cardiol 2004;44(4):733–9.
[5] Newby AC, Zaltsman AB. Molecular mechanisms in intimal hyperplasia. J Pathol 2000;190:300–9.
[6] Moussa I, Leon M, Baim D. Impact of sirolimus-eluting stents on outcome in diabetic patients: a SIRIUS substudy. Circulation 2004;109:2273–8.
[7] Stone G, Ellis S, Cox D, Hermiller J, O'Shaughnessy C, Mann J, et al. One-year clinical results with slow-release, polymer-based, paclitaxel-eluting TAXUS stent: the TAXUS-IV trial. Circulation 2004;109(16):1942–7.
[8] Finn AV, Nakazawa G, Joner M, Kolodgie FD, Mont EK, Gold HK, et al. Vascular responses to drug eluting stents: importance of delayed healing. Arterioscler Thromb Vasc Biol 2007;27(7):1500–10.
[9] Ong ATL, McFadden EP, Regar E, deJaegere PPT, vanDomburg RT, Serruys PW. Late angiographic stent thrombosis (LAST) events with drug-eluting stents. J Am Coll Cardiol 2005;45(12):2088–92.
[10] Iakovou I, Schmidt T, Bonizzoni E, Ge L, Sangiorgi G, Stankovic G, et al. Incidence, predictors, and outcome of thrombosis after successful implantation of drug-eluting stents. JAMA 2005;293(17):2126–30.
[11] Virmani R, Guagliumi G, Farb A, Musumeci G, Grieco N, Motta T, et al. Localized hypersensitivity and late coronary thrombosis secondary to a sirolimus-eluting stent: should we be cautious? Circulation 2004;109(6):701–5.
[12] Virmani R, Kolodgie F, Farb A. Drug-eluting stents: are they really safe? Am Heart Hosp J 2004;2(2):85–8.
[13] Virmani R, Farb A, Guagliumi G, Kolodgie F. Drug-eluting stents: caution and concerns for long-term outcome. Coron Artery Dis 2004;15(6):313–8.
[14] Nebeker JR, Virmani R, Bennet CL, Hoffman JM, Samore MH, Alvarez J, et al. Hypersensitivity cases associated with drug-eluting coronary stents: a review of available cases from the research on adverse drug events and reports (RADAR) project. J Am Coll Cardiol 2006;47(1):182–3.
[15] Mani G, Feldman MD, Patel D, Agrawal CM. Coronary stents: a materials perspective. Biomaterials 2007;28:1689–710.
[16] Wieneke H, Dirsch O, Sawitowski T, Gu YL, Brauer H, Dahmen U, et al. Synergistic effects of a novel nanoporous stent coating and tacrolimus on intima proliferation in rabbits. Catheter Cardiovasc Interv 2003;60(3):399–407.
[17] Wessely R, Hausleiter J, Michaelis C, Jaschke B, Vogeser M, Milz S, et al. Inhibition of neointima formation by a novel drug-eluting stent system that allows for dose-adjustable, multiple, and on-site stent coating. Arterioscler Thromb Vasc Biol 2005;25(4):748–53.
[18] Bhargava B, Reddy NK, Karthikeyan G, Raju R, Mishra S, Singh S, et al. A novel paclitaxel-eluting porous carbon-carbon nanoparticle coated, nonpolymeric cobalt–chromium stent: evaluation in a porcine model. Catheter Cardiovasc Interv 2006;67(5):698–702.
[19] Rajtar A, Kaluza GL, Yang Q, Hakimi D, Liu D, Tsui M, et al. Hydroxyapatite-coated cardiovascular stents. EuroIntervention 2006;2(1):113–5.
[20] Morice MC, Bestehorn HP, Carrié D, Macaya C, Aengevaeren W, Wijns W, et al. Direct stenting of de novo coronary stenoses with tacrolimus-eluting versus carbon-coated carbostents. The randomized JUPITER II trial. EuroIntervention 2006;2(1):45–52.
[21] Tsujino I, Ako J, Honda Y, Pj F. Drug delivery via nano-, micro and macro-porous coronary stent surfaces. Expert Opin Drug Deliv 2007;4(3):287–95.
[22] Mani G, Johnson DM, Marton D, Feldman MD, Patel D, Ayon A, et al. Drug delivery from gold and titanium surfaces using self assembled monoayers. Biomaterials 2008;29(34):4561–73.
[23] Mani G, Chandrasekar B, Feldman MD, Patel D, Agrawal CM. Interaction of endothelial cells with self assembed monolayers for potential use in drug eluting coronary stents. J Biomed Mater Res B Appl Biomater 2009;90(2):789–801.
[24] Wieczorek A, Vorpahl M, Mannhold R, Vogeser M, Hausleiter J, Joner M, et al. The pre-clinical assessment of rapamycin-eluting, durable polymer-free stent coating concepts. Biomaterials 2009;30(4):632–7.
[25] Van der Giessen WJ, Sorop O, Serruys PW, Peters-Krabbendam I, van Beusekom HM. Lowering the dose of sirolimus, released from a nonpolymeric hydroxyapatite coated coronary stent, reduces signs of delayed healing. JACC Cardiovasc Interv 2009;2(4):284–90.
[26] O'Brien B, Carroll W. The evolution of cardiovascular stent materials and surfaces in response to clinical drivers: a review. Acta Biomater 2009;5(4):945–58.
[27] Kollum M, Farb A, Schreiber R, Terfera K, Arab A, Geist A, et al. Particle debris from a nanoporous stent coating obscures potential antiproliferative effects of tacrolimus-eluting stents in a porcine model of restenosis. Catheter Cardiovasc Interv 2005;64(1):85–90.
[28] Carter AJ, Wamhoff B, Brodeur A, Christians U, Tio F, Lye WK, et al. Pharmacokinetics and pharmacodynamics of stent-based delivery of sirolimus via a novel metallic anisotropic nanoporous surface coating. Circulation 2006;114:II_511–2.
[29] Taylor A. Metals. In: Sigwart U, editor. Endoluminal stenting. London: W.B. Saunders Company Ltd; 1996. p. 28–33.
[30] Foti R, Tamburino C, Galassi A, Russo G, Nicosia A, Grassi R, et al. Safety, feasibility and efficacy of a new single-wire stent in the treatment of complex coronary lesions: the angiostent. Cardiologia 1998;43(7):725–30.
[31] Trepanier C, Venugopalan R, Pelton AR. Corrosion resistance and biocompatibility of passivated NiTi. In: Yahia LH, editor. Shape memory implants. New York: Springer; 2000. p. 35–45.
[32] Kereiakes D, Cox D, Hermiller J, Midei M, Bachinsky W, Nukta E, et al. Usefulness of a cobalt chromium coronary stent alloy. Am J Cardiol 2003;92(4):463–6.
[33] Yahya AM, McElnay JC, D'Arcy PF. Drug sorption to glass and plastics. Drug Metabol Drug Interact 1988;6(1):1–45.

[34] Martens HJ, De Goede PN, Van Loenen AC. Sorption of various drugs in polyvinyl chloride, glass, and polyethylene-lined infusion containers. Am J Hosp Pharm 1990;47(2):369–73.
[35] Song D, Hsu LF, Au JL. Binding of taxol to plastic and glass containers and protein under in vitro conditions. J Pharm Sci 1996;85(1):29–31.
[36] Palmgren JJ, Monkkonen J, Korjamo T, Hassinen A, Auriola S. Drug adsorption to plastic containers and retention of drugs in cultured cells under *in vitro* conditions. Eur J Pharm Biopharm 2006;64(3):369–78.
[37] Liistro F, Bolognese L. Drug-eluting stents. Heart Drug 2003;3:203–13.
[38] Lee BH, Nam HY, Kwon T, Kim SJ, Kwon GY, Jeon HJ, et al. Paclitaxel-coated expanded polytetrafluoroethylene haemodialysis grafts inhibit neointimal hyperplasia in porcine models of graft stenosis. Nephrol Dial Transplant 2006;21(9):2432–8.
[39] Kamath K, Barry JJ, Miller KM. The taxus drug-eluting stent: a new paradigm in controlled drug delivery. Adv Drug Deliv Rev 2006;58:412–36.
[40] Kilpadi DV, Raikar GN, Liu J, Lemons JE, Vohra Y, Gregory JC. Effect of surface treatment on unalloyed titanium implants: spectroscopic analyses. J Biomed Mater Res 1998;40(4):646–59.
[41] Adden N, Gamble LJ, Castner DG, Hoffmann A, Gross G, Menzel H. Phosphonic acid monolayers for binding of bioactive molecules to titanium surfaces. Langmuir 2006;22(19):8197–204.
[42] Hutt DA, Leggett GJ. Influence of adsorbate ordering on rates of UV photooxidation of self-assembled monolayers. J Phys Chem 1996;100(16): 6657–62.
[43] Wang A, Tang H, Cao T, Salley SO, Ng KYS. In vitro stability study of organosilane self-assembled monolayers and multilayers. J Colloid Interface Sci 2005;291(2):438–47.
[44] Mani G, Johnson D, Marton D, Dougherty VL, Feldman MD, Patel D, et al. Stability of self assembled monolayers on titanium and gold. Langmuir 2008;24:6774–84.
[45] Mani G, Feldman MD, Oh S, Agrawal CM. Surface modification of cobalt–chromium–tungsten–nickel alloy using octadecyltrichlorosilanes. Appl Surf Sci 2009;255(11):5961–70.
[46] Nanci A, Wuest JD, Peru L, Brunet P, Sharma V, Zalzal S, et al. Chemical modification of titanium surfaces for covalent attachment of biological molecules. J Biomed Mater Res 1998;40(2):324–35.
[47] McFadden EP, Stabile E, Regar E, Cheneau E, Ong ATL, Kinnaird T, et al. Late thrombosis in drug-eluting coronary stents after discontinuation of antiplatelet therapy. Lancet 2004;364(9444):1519–21.
[48] Otsuka Y, Chronos N, Apkarian R, Robinson K. Scanning electron microscopic analysis of defects in polymer coatings of three commercially available stents: comparison of BiodivYsio, Taxus and Cypher stents. J Invasive Cardiol 2007;19 (2):71–6.
[49] Joner M, Finn A, Farb A, Mont E, Kolodgie F, Ladich E, et al. Pathology of drug-eluting stents in humans: delayed healing and late thrombotic risk. J Am Coll Cardiol 2006;48(1):203–5.
[50] Donyai P, Sewell GJ. Physical and chemical stability of paclitaxel infusions in different container types. J Oncol Pharm Pract 2006;12(4):211–22.
[51] Mastropaolo D, Camerman A, Luo Y, Brayer GD, Camerman N. Crystal and molecular structure of paclitaxel (taxol). Proc Natl Acad Sci U S A 1995;92 (15):6920–4.
[52] Lee IH, Park YT, Roh K, Chung H, Kwon IC, Jeong SY. Stable paclitaxel formulations in oily contrast medium. J Control Release 2005;102(2):415–25.
[53] Kim S, Kim JY, Huh KM, Acharya G, Park K. Hydrotropic polymer micelles containing acrylic acid moieties for oral delivery of paclitaxel. J Control Release 2008;132(3):222–9.
[54] Haidopoulos M, Turgeon S, Sarra-Bournet C, Laroche G, Mantovani D. Development of an optimized electrochemical process for subsequent coating of 316 stainless steel for stent applications. J Mater Sci Mater Med 2006;17:647–57.
[55] Sojitra P, Engineer C, Raval A, Kothwala D, Jariwala A, Kotadia H, et al. Surface enhancement and characterization of L-605 cobalt alloy cardiovascular stent by novel electrochemical treatment. Trends Biomater Artif Organs 2009;23 (2):55–64.
[56] Milosev I, Strehblow HH. The composition of the surface passive film formed on CoCrMo alloy in simulated physiological solution. Electrochim Acta 2003;48:2767–74.
[57] Hodgson AWE, Kurz S, Virtanen S, Fervel V, Coa O. Passive and transpassive behavior of CoCrMo in simulated biological solutions. Electrochim Acta 2004;49:2167–78.
[58] Gawalt ES, Avaltroni MJ, Koch N, Schwartz J. Self-assembly and bonding of alkanephosphonic acids on the native oxide surface of titanium. Langmuir 2001;17(19):5736–8.
[59] Silverman BM, Wieghaus KA, Schwartz J. Comparative properties of siloxane vs phosphonate monolayers on a key titanium alloy. Langmuir 2005;21 (1):225–8.
[60] Liggins RT, Hunter WL, Burt HM. Solid-state characterization of paclitaxel. J Pharm Sci 1997;86(12):1458–63.
[61] Hancock BC, Zografi G. Characteristics and significance of the amorphous state in pharmaceutical systems. J Pharm Sci 1997;86(1):1–12.
[62] Byrn S, Pfeiffer R, Ganey M, Hoiberg C, Poochikian G. Pharmaceutical solids: a strategic approach to regulatory considerations. Pharm Res 1995;12 (7):945–54.
[63] Cremers B, Biedermann M, Mahnkopf D, Bohm M, Scheller B. Comparison of two different paclitaxel-coated baloon catheters in the porcine coronary restenosis model. Clin Res Cardiol 2009;98(5):325–30.
[64] Heldman A, Cheng L, Jenkins G, Heller P, Kim D, Ware M, et al. Paclitaxel stent coating inhibits neointimal hyperplasia at 4 weeks in a porcine model of coronary restenosis. Circulation 2001;103(18):2289–95.
[65] Hong MK, Mintz GS, Lee CW, Song JM, Han KH, Kang DH, et al. Paclitaxel coating reduces in-stent intimal hyperplasia in human coronary arteries. A serial volumetric intravascular ultrasound analysis from the asian paclitaxel-eluting stent clinical trial (ASPECT). Circulation 2003;107:517–20.
[66] Loya MC, Park E, Chen LH, Brammer KS, Jin S. Radially arrayed nanopillar formation on metallic stent wire surface via radio-frequency plasma. Acta Biomater 2009;6(4):1671–7.